Available online at www.sciencedirect.com
ScienceDirect
European Journal of Medicinal Chemistry 41 (2006) 1405–1411
EUROPEAN JOURNAL OF MEDICINAL CHEMISTRY
http://www.elsevier.com/locate/ejmech

Original article

Synthesis and biological activity of 8-azapurine and pyrazolo[4,3-*d*]pyrimidine analogues of myoseverin

Vladimír Kryštof [a,*], Daniela Moravcová [b], Martina Paprskářová [a], Pascale Barbier [c], Vincent Peyrot [c], Alice Hlobilková [d], Libor Havlíček [a,b], Miroslav Strnad [a]

[a] *Laboratory of Growth Regulators, Faculty of Science, Palacký University & Institute of Experimental Botany AS CR, Šlechtitelů 11, 783 71 Olomouc, Czech Republic*
[b] *Isotope Laboratory, Institute of Experimental Botany AS CR, Vídeňská 1083, 142 20 Prague 4, Czech Republic*
[c] *FRE-CNRS 2737 (ISPDCT), Faculté de Pharmacie, Université de la Méditerranée, 27 Bd. Jean Moulin, 13385 Marseille Cedex 05, France*
[d] *Institute of Pathology, Laboratory of Molecular Pathology, Faculty of Medicine, Palacký University, Hněvotínská 3, 775 15 Olomouc, Czech Republic*

Received 20 March 2006; received in revised form 27 June 2006; accepted 3 July 2006
Available online 22 September 2006

Abstract

The trisubstituted purine myoseverin has been recently identified as a novel inhibitor of microtubule assembly. To analyze the effects of modifying its heterocyclic skeleton, we prepared 8-azapurine and pyrazolo[4,3-*d*]pyrimidine analogues of myoseverin and compared their biological activities. Rearrangement of nitrogen atoms in the heterocycle changes the affinity of the compounds to purified tubulin, as demonstrated by the results of polymerization assays, and affects the proliferation of cancer cell lines. Surprisingly, compound E2GG, a pyrazolo[4,3-*d*]pyrimidine analogue of myoseverin, displayed inhibitory activity towards both tubulin polymerization and the activity of cyclin-dependent kinases 1, 2 and 7. Such a dual specificity-inhibitor offers a starting point for developing a novel class of antiproliferative agents.

Keywords: Myoseverin; Purine; Tubulin; Cyclin-dependent kinase; Cytoskeleton

1. Introduction

Microtubule interfering agents (MIAs) constitute an important group of anticancer drugs. They bind directly to tubulin and/or microtubules, suppressing equilibration between free and polymerized tubulin and slowing the polymerization dynamics [1]. The correct movements of the chromosomes and their proper segregation to daughter cells during mitosis require enormously rapid dynamics, making cell division very sensitive to MIAs. Interference with tubulin and improper assembly of the mitotic spindle trigger the arrest of the cell cycle and consequent apoptosis [1,2]. Unfortunately, many MIAs exhibit high cytotoxicity, which is a limiting factor for their clinical applications. Therefore, development of novel drugs lacking undesired side effects is still a challenge for medicinal chemists.

Using a muscle cell differentiation screen, a novel MIA named myoseverin was recently discovered in a 2,6,9-trisubstituted purine library [3]. Myoseverin was shown to induce the reversible fission of multinucleated myotubes into mononucleated fragments. Immunofluorescent visualization of the cytoskeleton in cells revealed that only the microtubular network was disintegrated. Myoseverin was also found to inhibit polymerization of tubulin in vitro, which is probably the stimulus for fission of myotubes into individual fragments. Transcriptome analysis of treated cells indicated that myoseverin affects the expression of many growth factors, immunomodulatory, extracellular matrix remodeling factors, and stress response factors, which is consistent with the activation of

* Corresponding author. Tel.: +420 585 634 854; fax: +420 585 634 870.
E-mail address: krystof@prfholnt.upol.cz (V. Kryštof).

0223-5234/$ - see front matter © 2006 Elsevier Masson SAS. All rights reserved.
doi:10.1016/j.ejmech.2006.07.004

pathways involved in wound healing and tissue regeneration [3]. Comparison of its cellular activity with that of other MIAs', including taxol, vinblastine, nocodazole and colchicines, showed that myoseverin is selectively reversible and lacks the typically high cytotoxicity of these non-purine MIAs [4].

Subsequent structure–activity relationship studies of myoseverin derivatives revealed that 9-cyclohexyl substituted myoseverin B is a stronger inhibitor of microtubule assembly [4,5]. These studies also confirmed that positions C2 and N6 on the purine are critical for inhibiting muscle differentiation, so the compounds may find applications in muscle regeneration and stem cell techniques. 2,6-Bis[2-(4-methoxyphenyl) ethyl]-9-isopropylpurine, an inactive carba-analogue of myoseverin, was also prepared. However, the exocyclic amino groups of myoseverin were shown to be essential for its biological activity [6]. Further optimization of the myoseverin molecule culminated in the identification of triazines that contain similar structural motifs and display even higher affinity to tubulin [7,8]. Tubulyzine®, the most potent triazine MIA, was then found to significantly reduce myoblast cell death following transplantation when used for pretreatment of the cells [8]. Such a process may improve long-term transplantation success in the treatment of inherited skeletal muscle diseases [8].

In addition to the potential of myoseverin and tubulyzines for transplantations, their antiproliferative capacities are also attractive for anticancer therapy. The purine derivative myoseverin, lacking major problems of common MIAs, represents an optimal starting point for expanding our small compounds library of protein kinase inhibitors towards MIAs. Various purines, 8-azapurines and pyrazolo[4,3-*d*]pyrimidines with different substituent patterns were recently prepared and examined as novel cyclin-dependent kinase (CDK) inhibitors in our laboratory [9–11]. We therefore synthesized two novel analogues of myoseverin with 8-azapurine and pyrazolo[4,3-*d*] pyrimidine skeletons (Fig. 1), bearing the same substituents

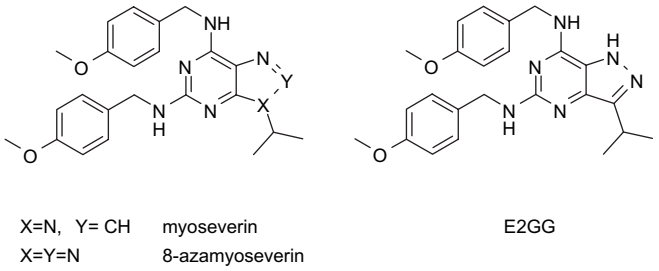

Fig. 1. Structures of myoseverin and its novel analogues 8-azamyoseverin and E2GG.

as myoseverin, and examined their effects in a tubulin polymerization assay in vitro. In addition, the antiproliferative activity of all three compounds was measured using several cancer cell lines. Surprisingly, one compound displayed inhibitory activity towards both tubulin polymerization and cyclin-dependent kinase activity.

2. Results and discussion

2.1. Synthesis

To prepare novel analogues of 2,6,9-trisubstituted purine myoseverin differing in the numbers and positions of nitrogen atoms in the heterocyclic skeleton, we had to develop completely new synthetic approaches. 3-Isopropyl-5,7-bis [(4-methoxybenzyl)amino]-1,2,3-triazolo[4,5-*d*]pyrimidine, designated 8-azamyoseverin, was synthesized from 3-isopropyl-5,7-dichloro-1,2,3-triazolo[4,5-*d*]pyrimidine and 4-methoxybenzylamine by recently described reactions [11]. The pyrazolo[4,3-*d*]pyrimidine analogue of myoseverin (E2GG) was prepared using a new synthetic route, outlined in Fig. 2. The carboxylic acid precursor (**1**) was synthesized according to Baraldi et al. [12]. After chlorination of **1** by $SOCl_2$ the chloro derivative was transformed to amide **2** with aqueous ammonia. Hydrogenation of the nitroamide produced the

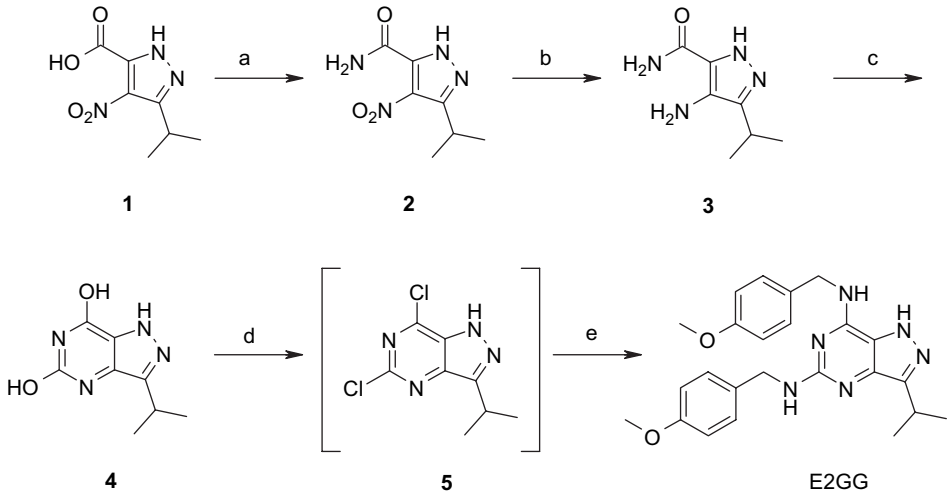

Fig. 2. Scheme of synthesis of 3,5,7-trisubstituted pyrazolo[4,3-*d*]pyrimidines. (a) 1. $SOCl_2$/reflux; 2. aq. NH_3, 76%; (b) RaNi, MeOH/H_2, 96%; (c) urea/180 °C, 78%; (d) $PhPOCl_2$/160 °C; (e) 4-methoxybenzylamine/145 °C, 38%.

aminoamide **3**. Fusing the amide with urea resulted in the dihydroxy derivative **4**. This derivative was then chlorinated with $PhPOCl_2$ giving 5,7-dichloro-3-isopropyl-1(2)*H*-pyrazolo[4,3-*d*]pyrimidine, a key precursor for the synthesis of trisubstituted pyrazolo[4,3-*d*]pyrimidines. The dichloro derivative **5** was immediately used for S_N (i.e. without an isolation step) with 4-methoxybenzylamine. The analogue of myoseverin E2GG was prepared in this way with 20% overall yield.

2.2. Effects on tubulin polymerization and CDK activity

The newly prepared analogues of myoseverin were checked for their ability to inhibit the polymerization of tubulin purified from lamb brain in vitro by a standard turbidimetric method [13,14]. Myoseverin has been previously shown to inhibit the polymerization of tubulin, with an IC_{50} of 8 μM [5]. This value corresponds very well with the results of our assay, 7 μM. Both 8-azamyoseverin and E2GG were also found to decrease the maximum turbidity of the reaction mixture in a dose-responsive manner, but with different efficiencies (Table 1). 8-Azamyoseverin inhibited the polymerization much less effectively than myoseverin. On the other hand, E2GG was found to be only slightly weaker as an MIA than myoseverin, with an IC_{50} of 16 μM. Neither myoseverin nor its novel analogues caused abnormal tubulin polymerization or aggregation when checked under the electronic microscope (data not shown).

Due to the structural similarity of myoseverin to 2,6,9-trisubstituted purine inhibitors of CDKs we also tested the compounds for possible CDK1/cyclin B kinase inhibition activity. Neither myoseverin itself nor 8-azamyoseverin had any inhibitory effect towards CDK1 (see Table 1 and Ref. [3]). Surprisingly, however, the pyrazolo[4,3-*d*]pyrimidine E2GG was able to block CDK1 activity with an IC_{50} value of 4.1 μM, a concentration equivalent to that of moderately potent inhibitors [9–11]. Furthermore, in vitro inhibitory effects were also seen towards recombinant CDK2/cyclin E ($IC_{50} = 3.7 \pm 1.0$ μM), CDK7/cyclin H ($IC_{50} = 7.2 \pm 2.5$ μM) and CDK9/cyclin T1 ($IC_{50} = 50.3 \pm 0.8$ μM), enzymes sharing a high degree of homology with CDK1, especially within their active sites. The difference in the biochemical activity between E2GG and myoseverin is presumably connected with the shift of the heterocyclic nitrogen, which may alter the binding mode within the active site of CDKs. With respect to the electron density distribution of the skeleton, the inhibitor E2GG probably interacts differently with the hinge region F80-E81-F82-L83 of CDK2, and this may contribute to its affinity to certain CDKs. Such an effect has been shown for purine CDK inhibitors, e.g. 6-cyclohexylmethoxypurines bearing 2-anilino substituents [15]. They bind to CDK2 in a manner different to that of classical purine CDK inhibitors, enabling the unsubstituted N9 to H-bond to the backbone carbonyl of E81.

Table 1
In vitro inhibition of lamb brain purified tubulin polymerization and CDK1 activity

Compound	Tubulin inhibition IC_{50} (μM)	CDK1 inhibition IC_{50} (μM)
Myoseverin	7.0 ± 0.8	~50
8-Azamyoseverin	50 ± 10	>40
E2GG	16 ± 2	4.1 ± 1.3
Colchicine	2.0 ± 0.4	>50

Values are means of two independent experiments ± SD.

2.3. Antiproliferative activity

Antiproliferative activity of myoseverin and its novel analogues was evaluated using several cancer cell lines of different histopathological origins. The data presented in Table 2 clearly show that myoseverin is active against all the tested cancer cell lines. Newly prepared 8-azamyoseverin displayed activity only towards four cell lines, three of which are also the most sensitive to the parental myoseverin. The other cell lines responded only marginally to 8-azamyoseverin at concentrations lower than 40 μM. By contrast, compound E2GG, a new pyrazolo[4,3-*d*]pyrimidine analogue of myoseverin, was much more active towards all the tested cell lines, even though its affinity to tubulin was somewhat lower than that of myoseverin. It blocked proliferation of most of the cell lines equally. Interestingly, its selectivity pattern was distinct from that of myoseverin; for example, the myoseverin-sensitive leukemia cell line HL60 grew approximately twice as fast in the presence of E2GG, and conversely the breast carcinoma line BT474 was about five times more sensitive to E2GG than to myoseverin. In addition, E2GG was screened towards 60 cancer cell lines at the National Cancer Institute, with the average GI_{50} value of 4.4 μM. The compound also showed activity in cell lines, which are resistant to some MIAs; for example, in neuronal SF-295 cells and breast NCI/ADR-RES the GI_{50} values are 3.2 μM and 3.5 μM, respectively. In summary, the results of the cellular

Table 2
In vitro antiproliferative activities of myoseverin and its novel analogues in human cancer cell lines

Cell line	IC_{50} (μM)		
	Myoseverin	8-Azamyoseverin	E2GG
A431	29.1 ± 0.1	>40	6.9 ± 0.2
A549	35.8 ± 4.1	>40	6.8 ± 0.4
BT474	35.8 ± 0.2	>40	$6.8 \pm .0.2$
CEM	6.2 ± 0.9	22.0 ± 6.6	6.3 ± 0.6
G361	24.0 ± 5.7	>40	6.7 ± 0.2
HBL100	22.6 ± 3.2	>40	6.4 ± 0.1
HeLa	10.6 ± 0.9	24.9 ± 7.1	5.2 ± 0.4
HL60	8.7 ± 3.3	38.2 ± 0.9	12.1 ± 3.7
HOS	30.8 ± 5.5	>40	9.2 ± 2.0
HS913T	31.5 ± 1.6	>40	8.4 ± 0.2
HT29	18.0 ± 8.7	>40	8.7 ± 0.1
K562	11.8 ± 2.6	>40	6.2 ± 0.2
MCF7	20.0 ± 4.6	>40	6.4 ± 0.5
SKUT1	33.8 ± 3.2	>40	8.1 ± 1.2
SVK14	8.0 ± 0.8	>40	5.8 ± 0.6
T98G	22.0 ± 4.0	32.8 ± 5.2	6.7 ± 0.5

Values are means of three experiments ± SD.

activity assays of all three compounds are consistent with the hypotheses that they inhibit tubulin polymerization, and that the microtubular cytoskeleton is their primary target in cells. Nevertheless, other cellular systems may also be affected by some of these compounds, as demonstrated by the affinity of E2GG to recombinant cyclin-dependent kinases and its slightly divergent cellular selectivity.

2.4. Flow cytometry and immunofluorescence

Antiproliferative activity of myoseverin is based on damage to the microtubular cytoskeleton [5]. We therefore verified the antiproliferative effects of novel myoseverin analogues by DNA flow cytometry analysis and indirect immunofluorescent detection of the microtubular cytoskeleton in the HeLa cell line. By 12 h, a substantial number of cells (62.5%) treated with 10 μM myoseverin were arrested at G2/M phases (Fig. 3B). They developed a rounded shape and contained substantially shortened microtubules compared with control cells (see Fig. 3F, and untreated cells shown in Fig. 3E). Similar effects were observed with 0.1 μM colchicine (data not shown). Surprisingly, 8-azamyoseverin, which had shown 7-fold lower potency against purified tubulin (Table 1) and lower antiproliferative activity than myoseverin (Table 2), also blocked a majority of HeLa cells at G2/M phases after 12 h incubation (Fig. 3C). Despite its strong influence on the cell cycle, 8-azamyoseverin displayed only marginal influence on microtubules (Fig. 3G), although it was applied in the same concentration as myoseverin. This discrepancy indicates that 8-azamyoseverin may exert its cell growth inhibitory effect through partial disruption or suppressed dynamics of microtubules or even through interactions with other cellular targets besides tubulin.

On the other hand, compound E2GG, which had also proved to be a slightly weaker MIA than myoseverin, caused similar damage to tubules after 12 h in HeLa cells, and to the same extent, as an equimolar dose of myoseverin (Fig. 3H). However, when the cells were subjected to flow cytometric analysis, only about a third of the population was found to be arrested in G2/M (Fig. 3D). We ascribe the diverse cellular effects to increased affinity of E2GG to other proteins, e.g. protein kinases. For example, cyclin-dependent kinase CDK1/cyclin B, which has been shown to be sensitive to E2GG (Table 1), phosphorylates several chromatin and cytoskeleton-associated proteins during mitosis and, thus, its inhibition leads to mitotic arrest [16]. The closely-related CDK2/cyclin E (which is also sensitive to E2GG) regulates G1/S transition and therefore its inhibition might be responsible for the increased G1 peak.

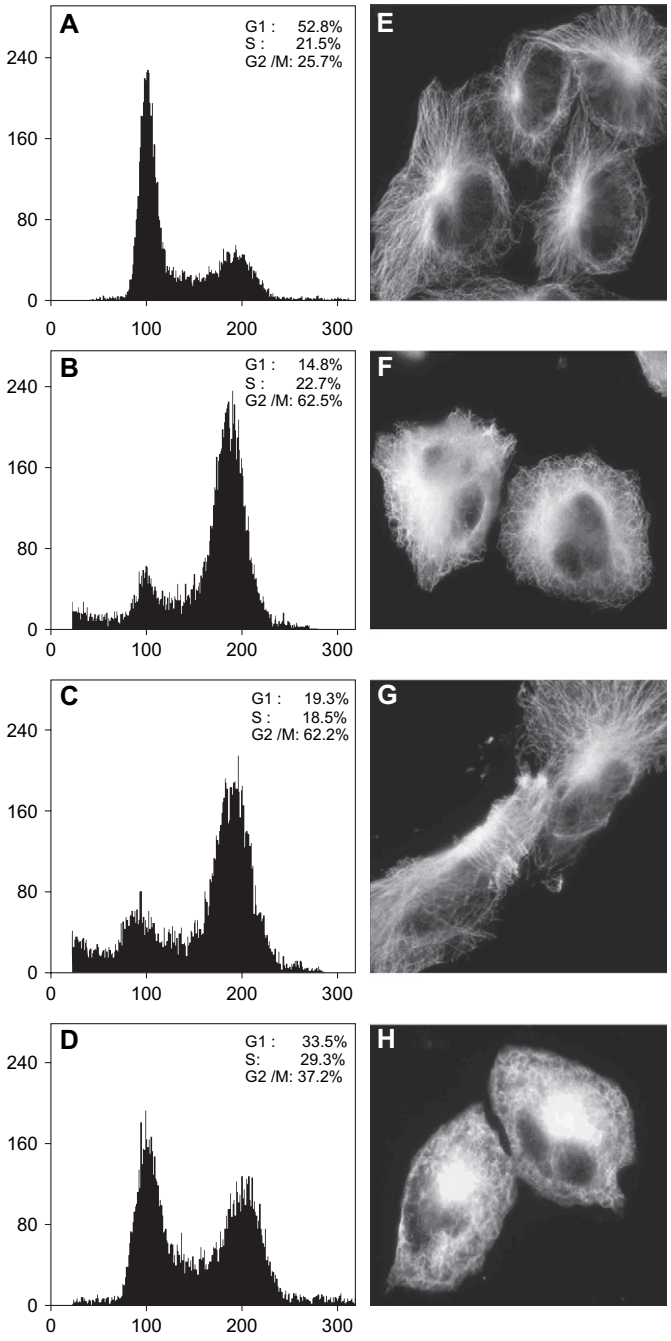

Fig. 3. Flow cytometric cell cycle analysis (A–D) and indirect immunofluorescent visualization of the microtubular cytoskeleton (E–F) of HeLa cells treated with the compounds (10 μM, 12 h). A, E: untreated cells; B, F: cells treated with myoseverin; C, G: cells treated with 8-azamyoseverin; D, H: cells treated with E2GG.

3. Conclusions

Compounds with stronger antiproliferative activity than the moderately active myoseverin could probably be identified by exploring structure–activity relationships. Therefore, two novel analogues of myoseverin were synthesized and assayed for their antiproliferative activities. 8-Azamyoseverin was found to be much weaker than myoseverin. On the other hand, pyrazolo[4,3-*d*]pyrimidines proved to offer a better scaffold not only for myoseverin-based MIAs, but also for other pharmacologically active compounds [10]. The unique dual specificity of E2GG, exceeding the antiproliferative activity of myoseverin, therefore represents an attractive starting point for further optimization. The dual targeting of E2GG here described may mirror its ability to mimic ATP binding with

CDK2, and probably GTP binding with tubulin, because the structurally similar substance tubulyzine B was recently suggested to localize within the GTP pocket of β-tubulin [17]. As demonstrated previously, combined anticancer chemotherapies using a CDK inhibitor and MIA could significantly improve their efficacy [18]. Further studies on the antiproliferative mechanisms of myoseverin and E2GG are underway.

4. Experimental

4.1. Chemicals

Colchicine was obtained from MP Biomedicals. Myoseverin was synthesized and characterized according to a published method [19]. Stock solutions for bioassays were prepared in DMSO and stored at 2 °C. The highest concentrations of DMSO in the polymerization buffer and the culture medium were 5% and 0.5%, respectively.

4.2. General experimental procedures

NMR spectra were measured using a Varian^{UNITY} Inova-400 spectrometer or a Varian Gemini-300 at 303 K. The residual solvent signal was used as an internal standard. ^{1}H NMR, ^{13}C NMR, COSY, TOCSY, HMQC, and HMBC spectra were analysed using the manufacturer's software (Varian Inc.). ^{1}H NMR spectra were zero-filled and exponential multiplication was applied prior Fourier transformation. Protons were assigned by COSY and TOCSY and the assignments were transferred to carbons by HMQC. Chemical shifts are given in δ-scale [ppm] and coupling constants in Hz. Carbon chemical shifts were read out from HMQC (protonated carbons) and HMBC. Mass spectra were determined using a Waters Micromass ZMD mass spectrometer (direct inlet, ESI, coin voltage 20 V); standard electron ionization EI mass spectra were recorded using a Jeol D100 double-focusing mass spectrometer (ionization energy 75 eV, chamber temperature 200 °C, ionizing current 300 mA, accelerating voltage 3 kV). All compounds gave satisfactory elemental analyses (0.4%). Merck silica gel Kieselgel 60 (230–400 mesh) was used for column chromatography.

4.3. Prepared compounds

4.3.1. 3-Isopropyl-5,7-bis[(4-methoxybenzyl)amino]-1,2,3-triazolo[4,5-d]pyrimidine (8-azamyoseverin)

A reaction mixture containing 5,7-dichloro-3-isopropyl-1,2,3-triazolo[4,5-*d*]pyrimidine (1.68 mmol) in 7 ml 1-butanol with 4-methoxybenzylamine (11.5 mmol) was stirred (110 °C, 17 h) according to a previously described procedure [11]. Crystals of the product were filtered; recrystallization from $CHCl_3$ afforded the product; yield 50%; mp 162–165 °C, ESI^{+}MS: 434.3 (100, $M+H^{+}$); ^{1}H NMR (400 MHz, $CDCl_3$): 1.65 (6H, d, $J = 6.8$ Hz, H-2″), 3.79 (3H, s, CH_3O'), 3.80 (3H, s, CH_3O), 4.60 (2H, d, $J = 5.7$ Hz, CH_2), 4.71 (2H, m, CH_2'), 4.95 (1H, septet, $J = 6.8$ Hz, H-1″), 5.52 (1H, br s, 2-NH), 6.53 (1H, br s, 6-NH′), 6.85 (2H, m, H′-*meta*), 6.86 (2H, m, H-*meta*), 7.27 (2H, m, H′-*ortho*), 7.29 (2H, m, H-*ortho*). ^{13}C NMR (100.55 MHz, $CDCl_3$, 303 K): 21.5 (C-2″), 43.7 (CH_2'), 45.2 (CH_2), 49.7 (C-1″), 55.0 ($2 \times OCH_3$), 113.8 (C-*meta*, C′-*meta*), 128.9 (C-*ortho*), 129.1 (C′-*ortho*), 129.9 (C′-*ipso*), 131.3 (C-*ipso*), 149.9 (C-4), 154.3 (C-6), 158.6 (C-*para*), 158.8 (C′-*para*), 160.6 (C-2). Anal. ($C_{23}H_{27}N_7O_2$) C, H, N.

4.3.2. 5-Isopropyl-4-nitro-1(2)H-pyrazole-3-carboxamide (2)

5-Isopropyl-4-nitro-1(2)*H*-pyrazole-3-carboxylic acid (**1**), 12.5 g (62.76 mmol), was refluxed with 18 ml $SOCl_2$ for 2 h. Excess $SOCl_2$ was then evaporated under reduced pressure. The residue was dissolved in acetone and aqueous ammonia was added dropwise (at −5 °C), with stirring, until the reaction was complete. The mixture was treated with charcoal, filtered and the filtrate was evaporated. The residual material was crystallized from ethanol: yield 76%; mp 163–170 °C; ^{1}H NMR (300 MHz, CD_3OD): 1.39 (6H, d, $J = 7.1$ Hz, $(CH_3)_2$–CH), 3.64 (1H, sept, $J = 7.1$ Hz, $CH(CH_3)_2$), 6.85 (2 H, br s). ^{13}C NMR (300 MHz, CD_3OD): 21.8, 24.7, 133.9, 134.6, 148.6, 169.8. Anal. ($C_7H_{10}N_4O_3$) C, H, N.

4.3.3. 4-Amino-5-isopropyl-1(2)H-pyrazole-3-carboxamide (3)

5-Isopropyl-4-nitro-1(2)*H*-pyrazole-3-carboxamide (3 g, 15.138 mmol) (**2**) was hydrogenated at atmospheric pressure and ambient temperature on 1 g of Raney nickel (W5 activity) in 20 ml MeOH and 5 ml H_2O for 9 h. The product was crystallized from EtOAc. The rest of the product was obtained from mother liquor by chromatography on silica in $CHCl_3$–MeOH (93:7); overall yield 96%; mp 177–179 °C; ^{1}H NMR (400 MHz; CD_3OD): 1.31 (6H, d, $J = 7.5$ Hz, $(CH_3)_2$–CH), 3.06 (1H, sept, $J = 7.5$ Hz, $CH(CH_3)_2$), 6.98 (2H, br s), 7.12 (2H, br s). ^{13}C NMR (400 MHz, CD_3OD): 21.5, 24.0, 128.5, 137.1, 165.6, 172.3. Anal. ($C_7H_{12}N_4O$) C, H, N.

4.3.4. 3-Isopropyl-1(2)H-pyrazolo[4,3-d]-pyrimidin-5,7-diol (4)

A mixture of 4-amino-5-isopropyl-1(2)*H*-pyrazole-3-carboxamide (**3**) (770 mg, 4.58 mmol) and urea (1.4 g, 4.58 mmol) was fused at 180 °C for 30 min. After cooling, the solid residue was dissolved in 2.3 ml of aqueous 2 M NaOH. The boiling solution was acidified with glacial acetic acid and the warm solution was filtered. This solution was cooled to 5 °C and the product started to precipitate after a few minutes. The product (1.3 g) was recrystallized twice from hot water; yield 78.5%; mp 295–298 °C; ^{1}H NMR (300 MHz, DMSO-d_6): 1.21 (6H, d, $J = 6.6$ Hz, CH_3CH–), 3.17 (1H, sept, $J = 6.6$ Hz, CH_3CH–). ^{13}C NMR (300 MHz, DMSO-d_6, 303 K): 21.6 (C-2″), 25.5 (C-1′), 124.9 (7a), 137.6 (7b), 145.4 (3), 150.4 (7), 154.7 (5). EI MS: 194 (94; M+); 179 (100; $C_7H_7N_4O_2$); 162 (51); 136 (15); 123 (7); 95 (8); 81 (13); 54 (26); 43 (23). Anal. ($C_8H_{10}N_4O_2$) C, H, N.

4.3.5. N-5,N-7-Bis(4-methoxybenzyl)-{3-isopropyl-1(2)H-pyrazolo[4,3-d]pyrimidin-5,7-diamine} (E2GG)

3-Isopropyl-1(2)*H*-pyrazolo[4,3-*d*]pyrimidin-5,7-diol (**4**) (1.16 g, 5.974 mmol) was dissolved in $PhPOCl_2$ (3.3 ml) and the mixture was heated to 160 °C in a sealed ampoule for 8 h. The solution was evaporated in vacuum (bath temperature up to 100 °C) and the residue was cooled and poured on crushed ice. The aqueous solution was extracted with chloroform. The extracts were dried over Na_2SO_4. The evaporated residue, 4-methoxybenzylamine (1.2 ml) and 0.5 ml of Hünnig base, was stirred at 145 °C for 6 h. The reaction mixture was evaporated and the residue was chromatographed over silica; $CHCl_3$/MeOH/NH_4OH (98/1.8/0.2); yield 91%; mp 83–85 °C; ESI^+MS: 433.3 (100%, $M+H^+$); ^1H NMR (400 MHz, $CDCl_3$): 1.28 (6H, d, $J=7.0$ Hz, H-2″), 3.49 (1H, sept. $J=7.0$ Hz, H-1″), 3.70 (3H, s, CH_3O'), 3.73 (3H, s, CH_3O), 4.56 (2H, m, CH_2), 4.64 (2H, m, CH_2'), 6.72 (2H, m, H′-*meta*), 6.820 (2H, m, H-*meta*), 7.17 (2H, m, H′-*ortho*), 7.21 (2H, m, H-*ortho*) 7.47 (1H, br s, 5-NH), 8.72 (1H, br s, 7-NH′). ^{13}C NMR (400 MHz, $CDCl_3$, 303 K): 21.5 (C-2″), 44.0 (CH_2'), 45.4 (CH_2), 55.2 (C-1″), 77.0 ($2\times OCH_3$), 113.9 (C-*meta*, C′-*meta*), 128.8 (C-*ortho*), 129.1 (C′-*ortho*), 129.4 (C′-*ipso*), 130.8 (C-*ipso*), 150.4 (C-4), 158.6 (C-7), 158.8 (C-*para*), 158.9 (C′-*para*), 160.4 (C-5). Anal. ($C_{24}H_{28}N_6O_2$) C, H, N.

4.4. Preparation of lamb brain tubulin

Tubulin was purified from soluble lamb brain homogenate by ammonium sulfate fractionation and ion exchange chromatography according to the published method [13,20,21]. The protein was stored in liquid nitrogen. Its concentration was determined spectrophotometrically with a Perkin–Elmer Lambda 800 spectrophotometer assuming an extinction coefficient at 275 nm of $1.07\,l\,g^{-1}\,cm^{-1}$ in 0.5% SDS in neutral aqueous buffer or $1.09\,l\,g^{-1}\,cm^{-1}$ in 6 M guanidine hydrochloride.

4.5. Tubulin polymerization

Microtubule assembly was assayed in 20 mM sodium phosphate, 1 mM EGTA, 3.4 M glycerol, and 0.1 mM GTP, pH 6.95. The polymerization reaction (20 μM tubulin) was started by increasing the temperature from 4 to 37 °C and the mass of formed polymer was monitored in thermostated cuvettes by measuring turbidity at 350 nm in a Beckman DU 7400 spectrophotometer as described earlier [14]. IC_{50} values were interpolated from graphs showing the percentage of turbidity inhibition as a function of the concentration of the tested compounds.

4.6. Electron microscopy

Small aliquots of polymerization mixtures were adsorbed to carbon-coated Formvar films on copper grids, stained for 1 min in 2% uranyl acetate and observed using a JEOL 1200 electron microscope.

4.7. CDK inhibition assays

Human 6xHis-tagged cyclin B/CDK1 complex was produced in Sf9 insect cells co-infected with appropriate baculoviral constructs and assayed as described earlier [10,11,22]. The cells were harvested, lysed and the enzyme was purified on a NiNTA column (Qiagen) according to the manufacturer's instructions. The assay mixture contained 1 mg/ml histone (Sigma Type III-S), 15 μM ATP, 0.2 μCi [γ-^{33}P] ATP and the tested compound in a final volume of 10 μl in reaction buffer (50 mM Hepes, pH 7.4, 10 mM $MgCl_2$, 5 mM EGTA, 10 mM 2-glycerolphosphate, 1 mM NaF, 1 mM DTT and protease inhibitors). After 10 min, the incubations were stopped by adding 5% H_3PO_4 and spotted on P81 phosphocellulose paper (Whatman). After washing in 5% H_3PO_4, the kinase activity was measured by a BAS-1800 digital imaging analyzer (Fujifilm). CDK2/cyclin E, CDK7/cyclin H and CDK9/cyclin T1 were produced and assayed as described previously [22,23]. The kinase activity was expressed as a percentage of maximum activity; the IC_{50} values were determined by graphical analysis.

4.8. Antiproliferative assay

The cell lines (all purchased from the American Type Culture Collection and German Collection of Microorganisms and Cell Cultures) were maintained at 37 °C and 5% CO_2, in a DMEM supplemented with fetal bovine serum, glutamine, penicillin and streptomycin. For anticancer cytotoxicity estimations, the cells were seeded at appropriate density into each well of a 96 well plate, allowed to stabilize for 24 h and the tested compounds were added at various concentrations in triplicate. Treatment lasted for 72 h. At the end of this period, a Calcein AM solution (Molecular Probes) was added and allowed to enter the cells for 1 h. The fluorescence of viable cells was quantified using a Fluoroskan Ascent microplate fluorometer (Labsystems) and cytotoxic effective concentrations were expressed as IC_{50}'s derived from dose–response curves [11,22].

4.9. Cell cycle analysis

Cells treated with the test compounds were harvested 12 h post-treatment together with negative controls and fixed in an ice-cold methanol. Before the analyses, the cells were rehydrated and stained with DAPI (0.1 μm/ml). DNA content was measured using a PAS flow cytometer (Partec). Measurements were performed in duplicate on 10 000 cells.

4.10. Indirect immunofluorescent analysis

Cells grown on glass cover slips were fixed with ice-cold methanol–acetone (1:1), then air-dried and stored at −20 °C until they were analysed. Rehydrated cells on cover slips were blocked with 10% fetal bovine serum in PBS. Microtubule networks were probed using a monoclonal anti-α-tubulin antibody (clone DM1A) and visualized with an anti-mouse

IgG – Texas Red conjugate (Dako). Nuclei were then stained with 4′,6-diamidino-2-phenylindole (DAPI) and the slips were mounted for microscopic observation.

Acknowledgments

This work was supported by grants 301/05/0418 and 204/03/D231 from the Czech Science Foundation, and by grant MSM 6198959216 from the Czech Ministry of Education. The authors thank I. Doležalová for help with flow cytometry, M. Hajdúch for discussions, E. Friesnerová and O. Hustáková for cell culture maintenance, the protein biochemistry and assay development and screening group members at Cyclacel for performing the CDK2, CDK7 and CDK9 assays, and Sees-editing for English editing.

References

[1] M.A. Jordan, L. Wilson, Nat. Rev. Cancer 4 (2004) 253–265.
[2] L.G. Wang, X.M. Liu, W. Kreis, D.R. Budman, Cancer Chemother. Pharmacol. 44 (1999) 355–361.
[3] G.R. Rosania, Y.T. Chang, O. Perez, D. Sutherlin, H. Dong, D.J. Lockhart, P.G. Schultz, Nat. Biotechnol. 18 (2000) 304–308.
[4] O.D. Perez, Y.T. Chang, G. Rosania, D. Sutherlin, P.G. Schultz, Chem. Biol. 9 (2002) 475–483.
[5] Y.T. Chang, S.M. Wignall, G.R. Rosania, N.S. Gray, S.R. Hanson, A.I. Su, J. Merlie Jr., S.H. Moon, S.B. Sangankar, O. Perez, R. Heald, P.G. Schultz, J. Med. Chem. 44 (2001) 4497–4500.
[6] M. Hocek, I. Votruba, H. Dvořáková, Tetrahedron 59 (2003) 607–611.
[7] H.S. Moon, E.M. Jacobson, S.M. Khersonsky, M.R. Luzung, D.P. Walsh, W. Xiong, J.W. Lee, P.B. Parikh, J.C. Lam, T.W. Kang, G.R. Rosania, A.F. Schier, Y.T. Chang, J. Am. Chem. Soc. 124 (2002) 11608–11609.
[8] E. El Fahime, M. Bouchentouf, B.F. Benabdallah, D. Skuk, J.F. Lafreniere, Y.T. Chang, J.P. Tremblay, Biochem. Cell Biol. 81 (2003) 81–90.
[9] L. Havlíček, J. Hanuš, J. Veselý, S. LeClerc, L. Meijer, G. Shaw, M. Strnad, J. Med. Chem. 40 (1997) 408–412.
[10] D. Moravcová, V. Kryštof, L. Havlíček, J. Moravec, R. Lenobel, M. Strnad, Bioorg. Med. Chem. Lett. 13 (2003) 2989–2992.
[11] L. Havlíček, K. Fuksová, V. Kryštof, M. Orság, B. Vojtěšek, M. Strnad, Bioorg. Med. Chem. 13 (2005) 5399–5407.
[12] P.G. Baraldi, B. Cacciari, A. Leoni, M. Recanatini, M. Roberti, M. Rossi, S. Manfredini, V. Periotto, D. Simoni, Farmaco 46 (1991) 1337–1350.
[13] J.M. Andreu, M.J. Gorbunoff, J.C. Lee, S.N. Timasheff, Biochemistry 23 (1984) 1742–1752.
[14] P. Barbier, C. Gregoire, F. Devred, M. Sarrazin, V. Peyrot, Biochemistry 40 (2001) 13510–13519.
[15] T.G. Davies, J. Bentley, C.E. Arris, F.T. Boyle, N.J. Curtin, J.A. Endicott, A.E. Gibson, B.T. Golding, R.J. Griffin, I.R. Hardcastle, P. Jewsbury, L.N. Johnson, V. Mesguiche, D.R. Newell, M.E. Noble, J.A. Tucker, L. Wang, H.J. Whitfield, Nat. Struct. Biol. 9 (2002) 745–749.
[16] A. Fourest-Lieuvin, L. Peris, V. Gache, I. Garcia-Saez, C. Juillan-Binard, V. Lantez, D. Job, Mol. Biol. Cell. 17 (2006) 1041–1050.
[17] Y.J. Kim, D.L. Sackett, M. Schapira, D.P. Walsh, J. Min, L.K. Pannell, Y.T. Chang, Bioorg. Med. Chem. 14 (2006) 1169–1175.
[18] D.S. O'Connor, N.R. Wall, A.C. Porter, D.C. Altieri, Cancer Cell 2 (2002) 43–53.
[19] F. Franěk, V. Siglerová, L. Havlíček, M. Strnad, T. Eckschlager, E. Weigl, Collect. Czech. Chem. Commun. 67 (2002) 257–266.
[20] R.C. Weisenberg, G.G. Borisy, E.W. Taylor, Biochemistry 7 (1968) 4466–4479.
[21] J.C. Lee, R.P. Frigon, S.N. Timasheff, J. Biol. Chem. 248 (1973) 7253–7262.
[22] V. Kryštof, I.W. McNae, M.D. Walkinshaw, P.M. Fischer, P. Müller, B. Vojtěšek, M. Orság, L. Havlíček, M. Strnad, Cell. Mol. Life Sci. 62 (2005) 1763–1771.
[23] S.J. McClue, D. Blake, R. Clarke, A. Cowan, L. Cummings, P.M. Fischer, M. MacKenzie, J. Melville, K. Stewart, S. Wang, N. Zhelev, D. Zheleva, D.P. Lane, Int. J. Cancer 102 (2002) 463–468.